The Veterinary Journal 212 (2016) 58–64

Contents lists available at ScienceDirect

The Veterinary Journal

journal homepage: www.elsevier.com/locate/tvjl

Effects of sphingolipid extracts on the morphological structure and lipid profile in an in vitro model of canine skin

Santiago Cerrato [a], Laura Ramió-Lluch [a], Pilar Brazís [a], Dolors Fondevila [b], Sergi Segarra [c], Anna Puigdemont [d,*]

[a] UNIVET, Edifici Astrolabio, Avinguda Cerdanyola 92, 08173 Sant Cugat del Vallès, Barcelona, Spain
[b] Department of Animal Medicine and Surgery, Facultat de Veterinària, Edifici V, Universitat Autònoma de Barcelona, 08913 Bellaterra, Barcelona, Spain
[c] R&D Veterinary Division, Bioiberica SA, Francesc Macià 7, 08029 Barcelona, Spain
[d] Department of Pharmacology, Therapeutics and Toxicology, Facultat de Veterinària, Edifici V, Universitat Autònoma de Barcelona, 08913 Bellaterra, Barcelona, Spain

ARTICLE INFO

Article history:
Accepted 22 March 2016

Keywords:
Canine
Skin
Ceramides
Sphingolipids
Atopic dermatitis

ABSTRACT

Ceramides (CER) are essential sphingolipids of the stratum corneum (SC) that play an important role in maintaining cutaneous barrier function. Skin barrier defects occur in both human beings and dogs affected with atopic dermatitis, and have been associated with decreased CER concentrations and morphological alterations in the SC. The aim of the present study was to investigate the changes induced by three different sphingolipid extracts (SPE-1, SPE-2 and SPE-3) on the morphological structure and lipid composition of canine skin, using an in vitro model, whereby keratinocytes were seeded onto fibroblast-embedded collagen type I matrix at the air–liquid interface. Cell cultures were supplemented with SPE-1, SPE-2, SPE-3 or vehicle (control) for 14 days. The relative concentrations of lipids were determined by ultra-performance liquid chromatography coupled to mass spectrometry. The ultrastructural morphology of samples was examined by transmission electron microscopy. SPE-1 induced significant elevation in total CERs, CER[NS], CER[NDS], CER[NP], CER[AS], CER[AP], CER[EOS] and CER[EOP] subclasses, whereas SPE-2 induced a significant elevation in total CER, CER[AP] and CER[EOS] compared with control conditions. Ultrastructural analysis revealed an increase in lamellar-lipid structures in the SC of SPE-1-treated samples. The findings demonstrated that SPE-1 stimulates production of CERs, as shown by changes in lipid composition and ultrastructural morphology. Thus, SPE-1 contributes to the formation of a well-organised SC and represents a potential therapeutic target for improving skin barrier function in atopic dermatitis.

Introduction

The stratum corneum (SC) of the skin, the outermost layer of the epidermis, plays an important role in barrier function, by limiting the penetration of substances and pathogens, and restricting water movement into and out of the skin. The cornified cell envelope is located in the inner cytoplasmic membrane of corneocytes and is composed of a cross-linked protein layer, which provides structural and mechanical integrity to the cells (Nemes and Steinert, 1999; Candi et al., 2005) and confers a scaffold structure to the extracellular lamellar lipids (Bouwstra and Ponec, 2006). Assembly of the extracellular lamellar lipids is a crucial factor in maintaining permeability barrier function (Swartzendruber et al., 1987, 1989). Precursors of the extracellular lipid matrix, including phospholipids, glucosylceramides, sphingomyelin and cholesterol, are located in the lamellar granules of keratinocytes at the upper stratum spinosum and stratum granulosum, and originate from the Golgi apparatus (Downing et al., 1987; Candi et al., 2005; Feingold, 2007, 2011).

In human beings, the lipid matrix consists mainly of three lipid classes: ceramides (CER), fatty acids and cholesterol (Elias and Feingold, 1992). Ceramides, as the major constituent of extracellular lamellar lipids, play a key role in determining cutaneous barrier function and the water-holding capacity of the SC (Bouwstra and Ponec, 2006; Jungersted et al., 2008). Canine SC has a CER profile closely resembling that of human beings (Popa et al., 2010). These extremely complex skin CERs include numerous molecular subclasses consisting of a combination of sphingoid moieties, including sphingosine [S], dihydrosphingosine [DS], phytosphingosine [P] and 6-hydroxy-sphingosine [H], linked via an amide bond to a fatty acid moiety, which may be non-hydroxy [N], α-hydroxy [A], or ester-linked ω-hydroxy [EO]. At present, the following CER subclasses have

* Corresponding author. Tel.: + 34 93 5811747.
E-mail address: anna.puigdemont@uab.cat (A. Puigdemont).

http://dx.doi.org/10.1016/j.tvjl.2016.03.020

been reported: CER[AH], CER[ADS], CER[AP], CER[AS], CER[EOH], CER[EOP], CER[EOS], CER[NH], CER[NDS], CER[NP] and CER[NS] (Masukawa et al., 2008; van Smeden et al., 2011; t'Kindt et al., 2012).

CER deficiency of the SC appears to be responsible, at least in part, for the cutaneous skin barrier defect and is recognised in both human and canine atopic dermatitis (AD) (Reiter et al., 2009; Shimada et al., 2009; Yoon et al., 2011; Nishifuji and Yoon, 2013). The dog has been shown to be a suitable model of human AD, because the development of clinical and immunological alterations in the disease resembles those in human beings (Santoro et al., 2013). Canine AD is defined as a genetically predisposed inflammatory and pruritic skin disease associated with immunoglobulin E antibodies against environmental and/or food allergens (Pucheu-Haston et al., 2015).

In canine AD, impaired cutaneous barrier function is associated with an increase in transepidermal water loss (TEWL) and, consequently, a reduction in skin hydration (Marsella and Samuelson, 2009; Hightower et al., 2010; Marsella et al., 2011). Increased TEWL has been associated with decreased CER levels and, in humans affected with AD, CER deficiency can be either a primary defect, the consequence of skin inflammation or both (Shimada et al., 2009; Santoro et al., 2015). Abnormalities of SC morphology have also been reported in skin from AD-affected dogs, as demonstrated by corneocyte disorganisation with wider intercellular spaces alongside an abnormal or incomplete lipid lamellae structure (Inman et al., 2001; Piekutowska et al., 2008; Marsella et al., 2010). There is increasing evidence that such defects might lead to excessive penetration by allergens and/or microorganisms, triggering an inflammatory process that can become chronic (Inman et al., 2001; Piekutowska et al., 2008; Ishida-Yamamoto et al., 2011). Recent studies have shown improvements in skin barrier function in dogs affected with canine AD following topical application and oral feed supplementation of preparations containing CERs, free fatty acids and cholesterol (Piekutowska et al., 2008; Popa et al., 2011, 2012; Jung et al., 2013).

In vitro models, known as skin equivalents (SEs), have been developed as an alternative to use of experimental animals. These bioengineered tissue substitutes consist of a dermal compartment, mainly consisting of collagen, which acts as a scaffold for primary cells of the epidermis (keratinocytes) and dermis (fibroblasts), thus replicating the cellular and structural properties of skin. SEs have been widely used in human skin biology research (Boyce and Williams, 1993; MacNeil, 2007), cutaneous irritation studies, toxicity testing (Welss et al., 2004; Park et al., 2010) and experimental modelling to test permeability and cutaneous absorption of different agents and formulations (Batheja et al., 2009; Tokudome et al., 2010). Although less well characterised, canine SE models have been developed (Barnhart et al., 2005; Magnol et al., 2005; Serra et al., 2007) and a canine SE model was validated for assessing the effects of topical oil formulations on skin morphology, functionality and changes in lipid composition (Cerrato et al., 2013). The aim of the present study was to investigate epidermal and dermal morphological structure and lipid profile composition in canine SEs exposed a number of lipid extracts rich in sphingolipids.

Materials and methods

Sphingolipid extracts

Three treatments were evaluated: sphingolipid extracts (SPE) 1–3 (Bioiberica SA). Each extract demonstrated a different lipid profile, but all were of animal origin. Compounds were emulsified in phosphate buffered saline (PBS) without Ca^{2+} or Mg^{2+} to 0.1% (W/V) and serially diluted to the desired concentration.

Isolation and culture of canine skin cells

Dermal fibroblasts and keratinocytes were isolated from biopsies obtained from the abdominal skin of healthy dogs after routine surgeries unrelated to the present study. Biopsies were collected in the Veterinary Hospital of the Universitat Autònoma de Barcelona (UAB), after obtaining informed written consent from the owner. All experimental protocols were supervised and approved by the Animal Ethics Committee of the UAB.

Skin samples were cleaned, cut into small fragments and enzymatically dispersed as previously described (Llames et al., 2006; Cerrato et al., 2013). Skin fragments were incubated with 2 mg/mL collagenase type I solution (Sigma-Aldrich) in Dulbecco's Minimal Essential Medium (DMEM, Invitrogen) for 4–6 h at 37 °C until the dermis was totally digested. The cell-rich supernatant was centrifuged at 300 *g* for 5 min, washed with PBS and the resulting fibroblasts were incubated in a humidified atmosphere at 37 °C with 5% CO_2 in culture medium consisting of DMEM supplemented with 10% foetal bovine serum (FBS) and antibiotics (Invitrogen).

The remaining epidermal fragments were subsequently washed and digested with a solution of 0.05% trypsin and 0.02% ethylene diamine tetraacetic acid (EDTA; Invitrogen) for 30 min at 37 °C to obtain keratinocytes. These were filtered twice with cell strainers (100 μm and 40 μm pore size, respectively; BD Biosciences) and centrifuged at 300 *g* for 5 min to recover the cells. Keratinocytes were seeded onto collagen-coated flasks and cultured in a humidified atmosphere at 37 °C with 5% CO_2 in DMEM/F12 (3:1) (Invitrogen) supplemented with 10% FBS, 0.01 g/mL epidermal growth factor (Austral Biologicals), 5 g/mL insulin, 7 ng/mL cholera toxin, 0.4 g/mL hydrocortisone, 1.3 ng/mL triiodothyronine, 24 g/mL adenine (Sigma-Aldrich) and antibiotics. Culture medium was changed every 2–3 days and cells were used for the SE model between the second and fifth passages.

Skin equivalent model

To obtain a three-dimensional SE, a collagen gel biomatrix was developed in a transwell chamber (Corning) by adding 4×10^4/mL mature fibroblasts to a 1.5 mg/mL type I collagen solution (Sigma-Aldrich) (Cerrato et al., 2013). The collagen gel biomatrix was cultured for 5–7 days, when 5×10^5 keratinocytes were seeded onto it. After 24 h, SEs were lifted to the air–liquid interface and the medium was modified by including 1% FBS, 0.1% L-serine, free fatty acids (15 μM linoleic acid, 7 μM arachidonic acid and 25 μM palmitic acid), 50 μg/mL ascorbic acid, 1 μM DL-α-tocopherol-acetate and 2.4×10^{-5} M bovine serum albumin (Sigma-Aldrich). SEs were cultured for 48 h before replacing the medium with medium lacking FBS but with additional 30 μM linoleic acid.

On the third day after seeding the keratinocytes, SEs were cultured in medium supplemented with SPE-1, SPE-2, SPE-3 or vehicle only. The final concentration of compounds in the culture medium was 0.001% (W/V). Skin equivalents were cultured over a total period of 14 days and medium and treatments were changed three times per week.

Histological and ultrastructural studies

SEs were fixed in 10% neutral buffered formalin, dehydrated in a graded series of ethanol and embedded in paraffin wax. Sections (4 μm) were stained using routine methods with haematoxylin and eosin (H&E) for histopathology. Ultrastructural studies were carried out by performing two different staining procedures. Firstly, samples were treated with paraformaldehyde–glutaraldehyde, then exposed to 1% (W/V) osmium tetroxide (TAAB) containing 0.8% (W/V) potassium hexacyanoferrate (III) (Sigma-Aldrich) for 2 h. Samples were dehydrated through a graded acetone series, embedded in Eponate 12 resin (Ted Pella) and polymerised for 48 h at 60 °C. Additionally, samples were treated with 2.5% glutaraldehyde, buffered in 0.1 M sodium cacodylate, then exposed to 0.2% ruthenium tetroxide in 0.1 M cacodylate (Sigma-Aldrich) for 1 h. After dehydration through a graded ethanol series up to 100% (W/V), samples were embedded in Spurr resin (Ted Pella) and polymerised for 48 h at 60 °C. Ultrathin sections (70 nm) from both staining procedures were cut with a diamond knife (45°; Diatome), mounted on copper grids (200 mesh) and contrasted with conventional uranyl acetate (30 min) and Reynold's lead citrate (5 min) solutions. Sections were visualised using a Jeol 1400 transmission electron microscope equipped with an Ultrascan ES1000 CCD camera (Gatan).

Lipid extraction and analysis

An ultra-performance liquid chromatography-mass/time-of-flight mass spectrometry (UPLC/TOF-MS) platform was used for profiling chloroform/methanol lipid extracts, providing coverage of glycerolipids, cholesteryl esters, sphingolipids and glycerophospholipids (Barr et al., 2012). Different treatments and SE samples were homogenised in the Precellys 24 homogeniser (Bertin Technologies) by mixing with chloroform/methanol (2:1, V/V) and sodium chloride (50 mM) (overall ratio 1:30:3, W/V/V), followed by protein precipitation. After brief vortexing, samples were incubated at –20 °C for 1 h. After centrifugation at 16,000 *g* for 15 min, the lower organic phase was collected and the solvent removed. The dried extracts were then resuspended in acetronitrile/isopropanol (1:1), centrifuged at 16,000 *g* for 5 min and supernatants were transferred to vials for UPLC-MS analysis on an Acquity-Xevo G2 Qtof mass spectrometry system (Waters Corporation). All UPLC analyses were performed in duplicate.

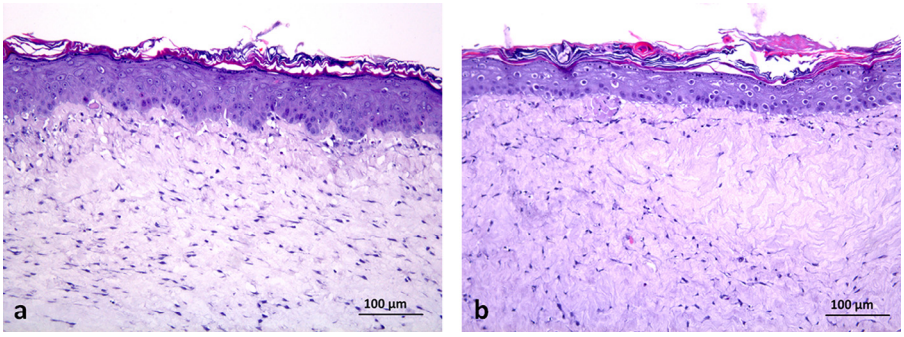

Fig. 1. Histological sections of (a) control and (b) sphingolipid extract (SPE)-1 treated canine skin equivalents. Haematoxylin and eosin stain.

Metabolite identification

Diacylglycerols (DAG), triacylglycerols (TAG), cholesteryl esters (ChoE), glycerophosphatidylethanolamines (PE), glycerophosphatidylcholines (PC), glycerophosphatidylinositols (PI), sphingomyelin (SM) and monohexosylceramides (CMH) were identified as described previously by Barr et al. (2012). The characterisation of the CER species (CER[ADS], CER[AH], CER[AP], CER[AS], CER[EOP], CER[EOS], CER[NDS], CER[NH], CER[NP] and CER[NS]) was carried out as described in detail by t'Kindt et al. (2012).

Data processing and statistical analysis

Data obtained with the UPLC-MS were processed with the TargetLynx application manager for MassLynx 4.1 (Waters Corporation), as described by Barr et al. (2012). Intra-batch and inter-batch normalisation followed the procedure detailed by van der Kloet et al. (2009). Univariate statistical analyses were performed to calculate group percentage changes and Student's *t* test, or Welch's *t* test where unequal variances were found, was applied to evaluate the effect of the treatments by comparing each treatment to the control. Statistical significance was set at $P < 0.05$. All calculations were performed with R v3.1.1 (R Development Core Team).

Results

Lipid profile of sphingolipid extracts

The lipid composition in the different treatment groups was analysed by UPLC-MS. Metabolite data analysis showed different lipid profiles for each treatment (Table 1). SPE-1 demonstrated the greatest sphingomyelin concentration and the least amount of CER, whereas SPE-2 showed relatively high levels of sphingomyelins, although to a lesser degree than SPE-1, and the greatest CER concentration. The greatest proportion of glycerolipids and glycerophospholipids was found in SPE-3.

Histology and ultrastructural analysis

SEs were produced successfully after 14 days culture at the air–liquid interface. On histological examination, differentiation and maturation of the dermal and epidermal compartments, as well as the dermo-epidermal junction, were observed in control and treated SEs (Fig. 1). Dermal fibroblasts were present in the matrix of collagen fibres and keratinocytes had differentiated into a stratified squamous keratinised epithelium (Fig. 1).

Ultrastructural analysis of the SC was performed by transmission electron microscopy after 14 days culture at the air–liquid interface. In both control and treated SEs, there was a thick, compact SC composed of different layers of corneocytes embedded in an intercellular lipid-enriched matrix (Fig. 2). Numerous lamellar bodies were observed at the border between the stratum granulosum and SC in SPE-1 treated samples and the intercellular spaces were filled with larger amounts of lipid material in some areas of the SC (Fig. 2). Ruthenium tetroxide staining of intercorneocyte spaces indicated the presence of intercellular lamellae that were well-organised in compact sheets. No other structural differences were observed when comparing control and treated samples (Fig. 3).

Table 1
Lipid composition of sphingolipid extracts; data are shown as percent contribution.

Lipid class	Treatments		
	SPE-1	SPE-2	SPE-3
Ceramides	0.81	26.70	11.63
Monohexosylceramides	0.32	0.04	0.06
Sphingomyelins	63.01	52.50	15.90
Monoacyl glycerols	0.06	0.04	0
Diacyl glycerols	4.16	10.67	0.91
Triacyl glycerols	1.41	18.98	36.22
Diacyl glycerophosphocholine	17.98	0.05	28.61
Monoether monoacyl phosphatidylcholine	1.74	0	6.61
Diacyl glycerophosphoethanolamine	0.60	0	0.05
Diacyl glycerophosphoinositol	0.06	0.02	0.01
Monoacyl glycerophosphocholine	9.85	0	0

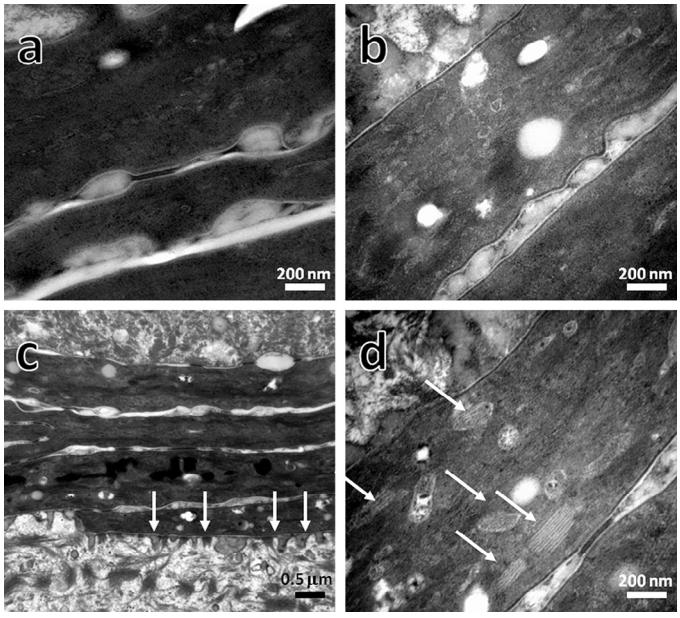

Fig. 2. Electron micrographs of the stratum corneum in (a) control and (b, c and d) sphingolipid extract (SPE)-1 treated canine skin equivalents. Samples were post-fixed with 1% osmium tetroxide and visualised by transmission electron microscopy. Numerous lamellar bodies can be observed at the stratum granulosum and stratum corneum border of SPE-1 treated samples (white arrows).

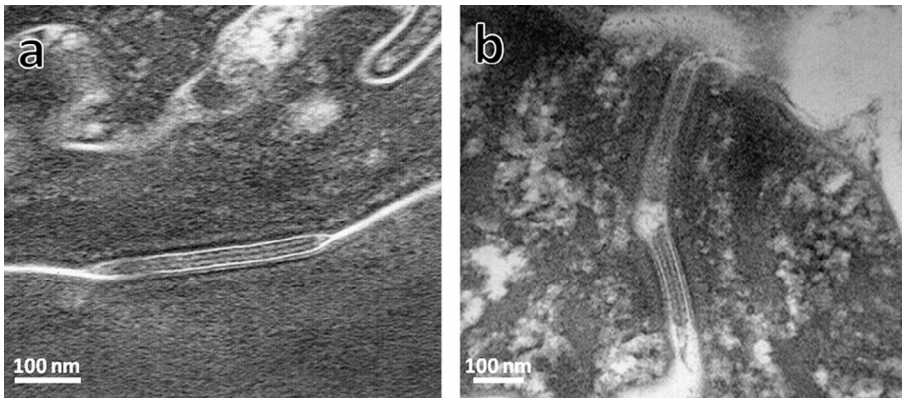

Fig. 3. Electron micrographs of lipid lamellae in (a) control samples and (b) sphingolipid extract (SPE)-1 treated canine skin equivalents. Normal lipid lamellae structures in alternating broad-narrow-broad lucent bands were observed in both control and treated samples. Samples were post-fixed with 0.2% ruthenium tetroxide.

Lipid profiles in canine skin equivalents exposed to sphingolipid extracts

To determine whether the lipid profile was modified in treated SEs when compared to controls, 307 skin lipid metabolites belonging to the glycerolipid group (DAG and TAG), sterol lipids (ChoE), glycerophospholipids (PE, PC and PI) and sphingolipids (CER, SM and CMH) were analysed by UPLC-MS. The relative concentration was calculated for each treatment group and compared with those from control tissues. The resulting data were arranged in a heat map, according to the carbon number and unsaturation degree of the esterified chains (Fig. 4).

In SPE-1 treated samples, there were significant increases in 44/99 (44.4%) CER metabolites when compared with controls; increased metabolites to CER[NS], CER[NDS], CER[NP], CER[AS], CER[AP], and CER[EOS] subclasses. There were no significant differences in CER metabolites in SPE-2 and SPE-3 treated samples compared with controls. There were no significant differences among groups in metabolites of glycerolipids, sterol lipids, glycerophospholipids or other sphingolipids.

Relative concentrations of total CERs and different CER subclasses are shown in Fig. 5. Total CER increased significantly after both SPE-1 and SPE-2 supplementation (2.2-fold and 2.1-fold, respectively). Likewise, CER[AP] and CER[EOS] subclasses also increased significantly after both SPE-1 (3.0-fold and 3.6-fold, respectively) and SPE-2 (2.2-fold and 3.0-fold, respectively) treatment, whereas CER[NS], CER[NDS], CER[NP], CER[AS] and CER[EOP] only increased after SPE-1 supplementation (2.2-fold, 2.2-fold, 2.1-fold, 2.4-fold and 1.9-fold, respectively). However, reductions in CER[NDS], CER[ADS], CER[AP] and CER[EOS] were observed in SPE-3 treatment samples (1.6-fold, 3.5-fold, 3.7-fold and 6-fold, respectively).

Discussion

In this study, a canine SE model was used to assess the effects of different sphingolipid extracts on lipid composition. There were significant increases in total CERs and CER[NS], CER[NDS], CER[NP], CER[AS], CER[AP], CER[EOS] and CER[EOP] subclasses after 2 weeks of SPE-1 treatment, while SPE-2 induced a significant increase in total CERs, CER[AP] and CER[EOS]. In contrast, a reduction in these CER subclasses has been demonstrated consistently in the SC in dogs with AD. Reiter et al. (2009) reported lower proportions of CER[EOS] and CER[EOP], whereas Yoon et al. (2011) found that total CERs, CER[EOS], CER[EOP], CER[NP] and mixtures of CER[NDS/NS] and CER[AS/NH] subclasses, were significantly lower in atopic dogs than unaffected dogs. In atopic dogs, Popa et al. (2011) reported reductions in protein-bound CER[OS] and CER[OP], which are degradation products of free extractable CER[EOS] and CER[EOP], respectively. Stahl et al. (2012) reported a decrease in total CER and CER[AH], CER[AP], CER[AS], CER[NP], CER[EOP], CER[NS] and CER[EOS] fractions in atopic Maltese-Beagle dogs after intradermal allergen challenge.

Similar alterations in CER composition have also been detected in other canine skin diseases. Yoon et al. (2013) indicated that quantities of some CER subclasses, including CER[EOS], CER[EOP], CER[OH] and a mixture of CER[AS/NH] were significantly lower in Shih Tzu dogs with seborrhoea than dogs without seborrhoea. A reduction in total CERs, and CER[NP], CER[EOS] and CER[EOP] subclasses, has also been reported in human AD (Di Nardo et al., 1998). Thus, the CER subclasses most widely reported to be reduced in canine and human AD, particularly CER[EOS] and CER[EOP], were increased after SPE-1 treatment.

Interestingly, CER[EOS] and CER[EOP], the esterified ω-hydroxyceramides with the largest carbon chains, are believed to be critical for normal SC barrier function and are important carriers of linoleic acid, which is also involved in the maintenance of the cutaneous water permeability barrier (Watson, 1998; Mizutani et al., 2009). On the basis of these findings, CER[EOS] and CER[EOP] are likely to represent the most relevant CER subclasses involved in the pathogenesis of skin barrier defects in AD, although other CER subclasses, such as short carbon chains CERs (CER[AP] and CER[NP]), may also play a role.

These changes in total CER and CER subclasses observed in skin samples after SPE-1 and SPE-2 treatment could be the result of direct CER incorporation from sphingolipid extracts. However, SPE-3 contained a greater proportion of CERs than SPE-1 and SEs treated with SPE-3 did not show a significant increase in total CERs or any CER subclass, unlike SPE-1 and SPE-2. Therefore, such treatments may be largely due to increased endogenous production, rather than the presence of CERs in the treatment per se. Furthermore, the relatively high content of sphingomyelins in SPE-1 and SPE-2, when compared with SPE-3, could be responsible for stimulating synthesis of CERs, since sphingomyelins are precursors of CER biosynthesis in the skin (Feingold, 2007).

Ultrastructural abnormalities have been reported in the SC of dogs affected with canine AD. Disorganisation of the lipid lamellae and a wider and emptier intercellular space between corneocytes have been reported in the SC of atopic dogs and horses (Inman et al., 2001; Piekutowska et al., 2008; Jung et al., 2013; Marsella et al., 2014). Marsella et al. (2010), using an experimental model for canine AD, also observed disorganisation of the extracellular lipid lamellae,

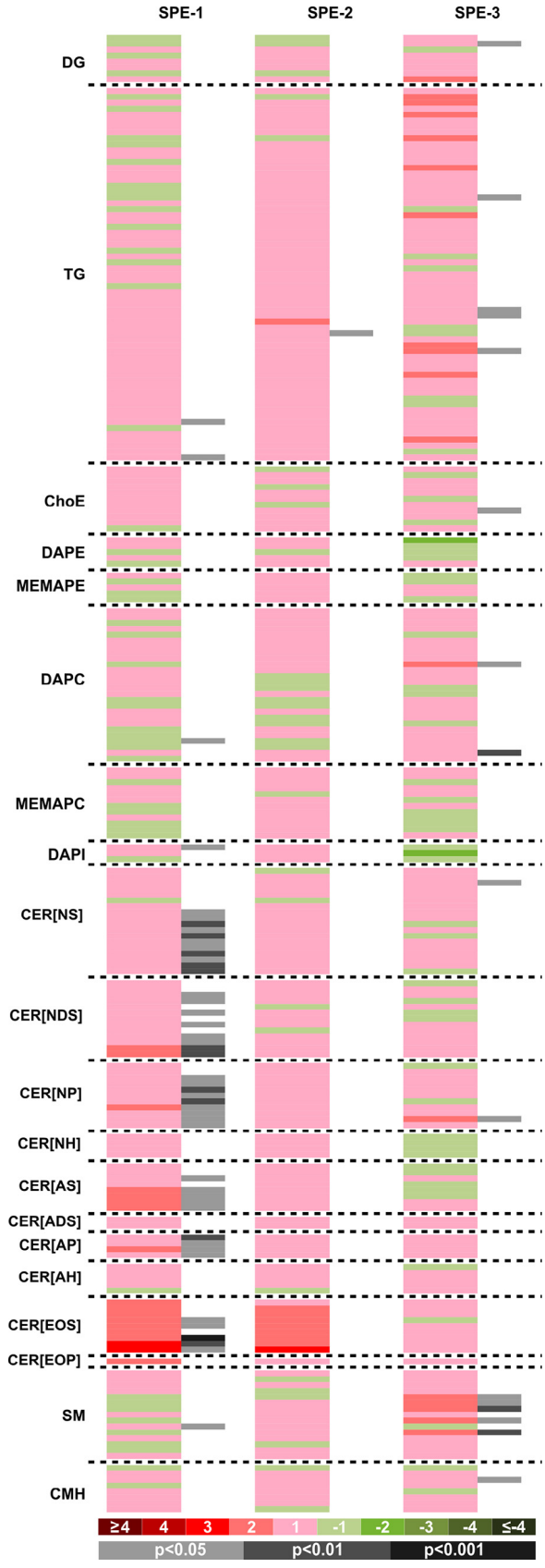

Fig. 4. Heat map showing lipid profile of different skin lipid metabolites obtained when comparing treatment groups (sphingolipid extracts: SPE-1, SPE-2 and SPE-3) with the control group. The first column of each comparison represents fold changes of increased (red colour scale) and decreased (green colour scale) metabolites, while the second column represents the, *P* values for each significant fold change (grey colour scale). Colour codes for magnitude of fold changes and *P* values are indicated.

increased width between corneocytes, lamellar bodies within corneocytes and large amounts of amorphous intercellular lipids.

Jung et al. (2013) demonstrated improvement in AD-affected dogs after topical treatment with preparations containing CERs, free fatty acids and cholesterol, demonstrating their efficacy in improving SC structure and also helping to reduce TEWL, pruritus and Canine Atopic Dermatitis Extent and Severity Index (CADESI) scores. Moreover, other studies of canine AD have reported an improvement in SC organisation and lipid content after dietary supplementation with ω-6/ω-3 fatty acids and topical sphingolipid-containing emulsion therapy (Popa et al., 2011).

The present study showed numerous SC lipid lamellar-related structures after SPE-1 treatment (intercorneocyte lipid fulfilment and lamellar bodies). Since the permeability and microbial barriers are maintained by lipids and proteins delivered to the extracellular spaces of the SC through the secretion of lamellar bodies (Feingold, 2012), an increase in the number of these structures in the SE model after treatment with SPE-1 might constitute a potential improvement in barrier function of the skin in dogs. Moreover, the electron micrographs revealed a clear trilaminar structure of lipid lamellae in altering broad-narrow-broad lucent bands. CER[EOS] is considered to play an important role in the formation and stabilisation of the trilaminar lipid structure, resulting in this characteristic pattern (Madison et al., 1987; Kuempel et al., 1998; Groen et al., 2010). Interestingly, CER[EOS] showed the greatest increase of all CER subclasses after SPE-1 treatment (3.6-fold), although this trilaminar structure was present in both the control and treated samples. Taking into account that the tissue model used in the present study was a 'healthy' SE model, one could speculate that the beneficial effects of this lipid-based treatment may be more evident in the SC of atopic patients deficient in CER[EOS].

Sphingolipids can be obtained from animal or plant sources and may also be produced from genetically modified microorganisms. Different commercial products containing sphingolipids are available, but most are plant-based. In mammals, most endogenous sphingolipids contain sphingosine, which is not present in plants. This compound is combined with fatty acid to form CERs. The most common sphingolipids in humans (sphingomyelin and galactosylceramides) are not present in plants (Sperling and Heinz, 2003). The sphingolipid extracts used in the present study were of animal origin and therefore they presented a lipid profile that was more suitable for endogenous synthesis of CERs.

The SE model recapitulates the cellular and structural properties of skin and is an alternative to the use of animals in research. The methodology described in the present study allows a canine SE model to be generated from cells readily available from small skin biopsies. The results obtained demonstrate that this technique is useful as a model to investigate the potential effects of lipid-based formulations on canine skin.

Conclusions

The findings of this study indicate that sphingolipid-based treatments may have a beneficial effect for improving the skin barrier. SPE-1 enhances endogenous production of CERs, contributing to the formation of a well-organised SC. This treatment has potential for use in skin diseases such as AD and seborrhoea, although clinical studies are needed to confirm these results and improve our understanding of the mechanisms involved.

Conflict of interest statement

Sergi Segarra is an employee of Bioiberica SA (R&D Veterinary Division) and participated in the design of the study and helped to

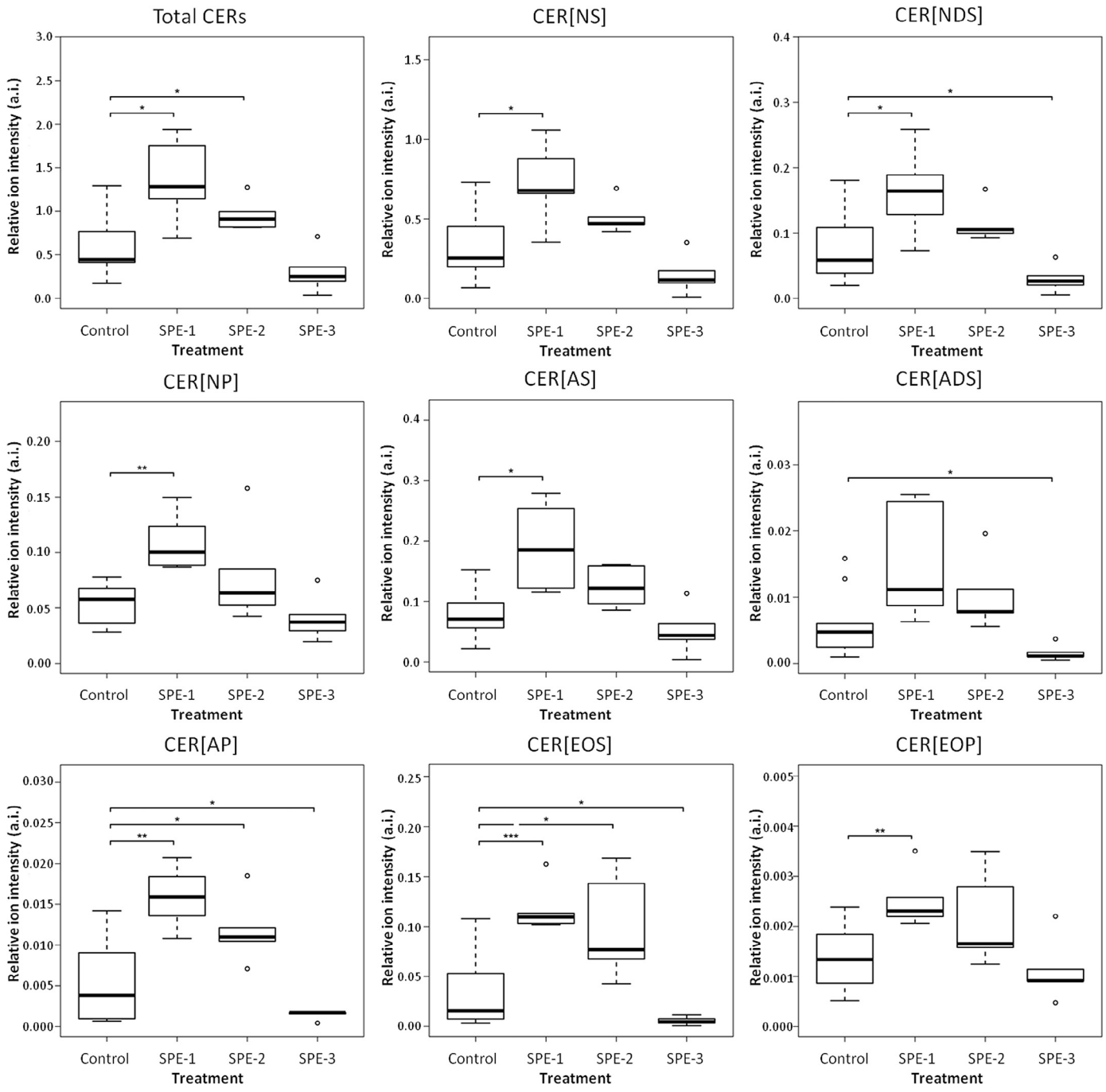

Fig. 5. Box plots of median relative quantities (bold horizontal lines) of total ceramides (CERs) and CER subclasses (CER[NS], CER[NDS], CER[NP], CER[AS], CER[ADS], CER[AP], CER[EOS] and CER[EOP]) in SPE1-3 treated and control skin equivalents (SEs). Bottom and top of the box correspond to the 25th and 75th percentiles, respectively. Whiskers correspond to maximum and minimum values. Circles represent outliers. $^{*}P < 0.05$ and $^{**}P < 0.001$ comparing SEs treated with sphingolipid extracts (SPE-1, SPE-2, SPE-3) to control SEs.

the draft of the manuscript. None of the other authors has any financial or personal relationships that could inappropriately influence or bias the content of the paper.

Acknowledgements

The authors gratefully acknowledge Dr Cristina Alonso for her invaluable help and technical support with UPLC-MS and Dr Alex Sanchez Chardi for his technical support with electron microscopy. This work was partially supported by Bioiberica SA.

References

Barnhart, K.F., Credille, K.M., Ambrus, A., Dunstan, R.W., 2005. Preservation of phenotype in an organotypic cell culture model of a recessive keratinization defect of Norfolk terrier dogs. Experimental Dermatology 14, 481–490.

Barr, J., Caballería, J., Martínez-Arranz, I., Domínguez-Díez, A., Alonso, C., Muntané, J., Pérez-Cormenzana, M., García-Monzón, C., Mayo, R., Martín-Duce, A., et al., 2012. Obesity-dependent metabolic signatures associated with nonalcoholic fatty liver disease progression. Journal of Proteome Research 11, 2521–2532.

Batheja, P., Song, Y., Wertz, P., Michniak-Kohn, B., 2009. Effects of growth conditions on the barrier properties of a human skin equivalent. Pharmaceutical Research 26, 1689–1700.

Bouwstra, J.A., Ponec, M., 2006. The skin barrier in healthy and diseased state. Biochimica et Biophysica Acta 1758, 2080–2095.
Boyce, S.T., Williams, M.L., 1993. Lipid supplemented medium induces lamellar bodies and precursors of barrier lipids in cultured analogues of human skin. Journal of Investigative Dermatology 101, 180–184.
Candi, E., Schmidt, R., Melino, G., 2005. The cornified envelope: A model of cell death in the skin. Nature Reviews. Molecular Cell Biology 6, 328–340.
Cerrato, S., Ramio-Lluch, L., Fondevila, D., Rodes, D., Brazis, P., Puigdemont, A., 2013. Effects of essential oils and polyunsaturated fatty acids on canine skin equivalents: Skin lipid assessment and morphological evaluation. Journal of Veterinary Medicine 2013, 231526.
Di Nardo, A., Wertz, P., Giannetti, A., Seidenari, S., 1998. Ceramide and cholesterol composition of the skin of patients with atopic dermatitis. Acta Dermato-Venereologica 1, 27–30.
Downing, D.T., Stewart, M.E., Wertz, P.W., Colton, S.W., Abraham, W., Strauss, J.S., 1987. Skin lipids: An update. Journal of Investigative Dermatology 88, 2s–6s.
Elias, P.M., Feingold, K.R., 1992. Lipids and the epidermal water barrier: Metabolism, regulation, and pathophysiology. Seminars in Dermatology 11, 176–182.
Feingold, K.R., 2007. Thematic review series: Skin lipids. The role of epidermal lipids in cutaneous permeability barrier homeostasis. Journal of Lipid Research 12, 2531–2546.
Feingold, K.R., 2011. Lipid metabolism in the epidermis. Dermato-endocrinology 3, 52.
Feingold, K.R., 2012. Lamellar bodies; the key to cutaneous barrier function. Journal of Investigative Dermatology 8, 1951–1953.
Groen, D., Gooris, G.S., Bouwstra, J.A., 2010. Model membranes prepared with ceramide EOS, cholesterol and free fatty acids form a unique lamellar phase. Langmuir: The ACS Journal of Surfaces and Colloids 6, 4168–4175.
Hightower, K., Marsella, R., Flynn-Lurie, A., 2010. Effects of age and allergen exposure on transepidermal water loss in a house dust mite-sensitized beagle model of atopic dermatitis. Veterinary Dermatology 21, 88–95.
Inman, A.O., Olivry, T., Dunston, S.M., Monteiro-Riviere, N.A., Gatto, H., 2001. Electron microscopic observations of stratum corneum intercellular lipids in normal and atopic dogs. Veterinary Pathology 38, 720–723.
Ishida-Yamamoto, A., Igawa, S., Kishibe, M., 2011. Order and disorder in corneocyte adhesion. Journal of Dermatology 38, 645–654.
Jung, J.Y., Nam, E.H., Park, S.H., Han, S.H., Hwang, C.Y., 2013. Clinical use of a ceramide-based moisturizer for treating dogs with atopic dermatitis. Journal of Veterinary Science 14, 199–205.
Jungersted, J.M., Hellgren, L.I., Jemec, G.B., Agner, T., 2008. Lipids and skin barrier function – a clinical perspective. Contact Dermatitis 58, 255–262.
Kuempel, D., Swartzendruber, D.C., Squier, C.A., Wertz, P.W., 1998. In vitro reconstitution of stratum corneum lipid lamellae. Biochimica Biophysic Acta 1, 135–140.
Llames, S., Garcia, E., Garcia, V., del Río, M., Larcher, F., Jorcano, J.L., López, E., Holguín, P., Miralles, F., Otero, J., et al., 2006. Clinical results of an autologous engineered skin. Cell and Tissue Banking 7, 47–53.
MacNeil, S., 2007. Progress and opportunities for tissue-engineered skin. Nature 445, 874–880.
Madison, K.C., Swartzendruber, D.C., Wertz, P.W., Downing, D.T., 1987. Presence of intact intercellular lipid lamellae in the upper layers of the stratum corneum. Journal of Investigative Dermatology 6, 714–718.
Magnol, J.P., Pin, D., Palazzi, X., Lacour, J.P., Gache, Y., Meneguzzi, G., 2005. Characterization of a canine model of dystrophic bullous epidermolysis (DBE). Development of a gene therapy protocol. Bulletin de l'Académie Nationale de Médecine 189, 107–121.
Marsella, R., Samuelson, D., 2009. Unravelling the skin barrier: A new paradigm for atopic dermatitis and house dust mites. Veterinary Dermatology 20, 533–540.
Marsella, R., Samuelson, D., Doerr, K., 2010. Transmission electron microscopy studies in an experimental model of canine atopic dermatitis. Veterinary Dermatology 21, 81–88.
Marsella, R., Olivry, T., Carlotti, D.N., 2011. Current evidence of skin barrier dysfunction in human and canine atopic dermatitis. Veterinary Dermatology 22, 239–248.
Marsella, R., Johnson, C., Ahrens, K., 2014. First case report of ultrastructural cutaneous abnormalities in equine atopic dermatitis. Research in Veterinary Science 2, 382–385.
Masukawa, Y., Narita, H., Shimizu, E., Kondo, N., Sugai, Y., Oba, T., Homma, R., Ishikawa, J., Takagi, Y., Kitahara, T., et al., 2008. Characterization of overall ceramide species in human stratum corneum. Journal of Lipid Research 49, 1466–1476.
Mizutani, Y., Mitsutake, S., Tsuji, K., Kihara, A., Igarashi, Y., 2009. Ceramide biosynthesis in keratinocyte and its role in skin function. Biochimie 6, 784–790.
Nemes, Z., Steinert, P.M., 1999. Bricks and mortar of the epidermal barrier. Experimental and Molecular Medicine 31, 5–19.
Nishifuji, K., Yoon, J.S., 2013. The stratum corneum: The rampart of the mammalian body. Veterinary Dermatology 1, 60–72.
Park, Y.H., Kim, J.N., Jeong, S.H., Choi, J.E., Lee, S.H., Choi, B.H., Lee, J.P., Sohn, K.H., Park, K.L., Kim, M.K., et al., 2010. Assessment of dermal toxicity of nanosilica using cultured keratinocytes, a human skin equivalent and an in vivo model. Toxicology 267, 178–181.
Piekutowska, A., Pin, D., Rème, C.A., Gatto, H., Haftek, M., 2008. Effects of a topically applied preparation of epidermal lipids on the stratum corneum barrier of atopic dogs. Journal of Comparative Pathology 138, 197–203.
Popa, I., Thuy, L.H., Colsch, B., Pin, D., Gatto, H., Haftek, M., Portoukalian, J., 2010. Analysis of free and protein-bound ceramides by tape stripping of stratum corneum from dogs. Archives of Dermatological Research 302, 639–644.
Popa, I., Pin, D., Remoué, N., Osta, B., Callejon, S., Videmont, E., Gatto, H., Portoukalian, J., Haftek, M., 2011. Analysis of epidermal lipids in normal and atopic dogs, before and after administration of an oral omega-6/omega-3 fatty acid feed supplement. A pilot study. Veterinary Research Communications 35, 501–509.
Popa, I., Remoue, N., Osta, B., Pin, D., Gatto, H., Haftek, M., Portoukalian, J., 2012. The lipid alterations in the stratum corneum of dogs with atopic dermatitis are alleviated by topical application of a sphingolipid-containing emulsion. Clinical and Experimental Dermatology 37, 665–671.
Pucheu-Haston, C.M., Bizikova, P., Eisenschenk, M.N., Santoro, D., Nutall, T., Marsella, R., 2015. The role of antibodies, autoantigens and food allergens in canine atopic dermatitis. Veterinary Dermatology 26, 115–e30.
Reiter, L.V., Torres, S.M., Wertz, P.W., 2009. Characterization and quantification of ceramides in the nonlesional skin of canine patients with atopic dermatitis compared with controls. Veterinary Dermatology 20, 260–266.
Santoro, D., Marsella, R., Ahrens, K., Graves, T.K., Bunick, D., 2013. Altered mRNA and protein expression of filaggrin in the skin of a canine animal model for atopic dermatitis. Veterinary Dermatology 3, 329–336.
Santoro, D., Marsella, R., Pucheu-Hatson, C.M., Eisenschenk, M.N., Nuttall, T., Bizikova, P., 2015. Review: Pathogenesis of canine atopic dermatitis: Skin barrier and host-micro-organism interaction. Veterinary Dermatology 2, 84–e25.
Serra, M., Brazís, P., Puigdemont, A., Fondevila, D., Romano, V., Torre, C., Ferrer, L., 2007. Development and characterization of a canine skin equivalent. Experimental Dermatology 16, 135–142.
Shimada, K., Yoon, J.S., Yoshihara, T., Iwasaki, T., Nishifuji, K., 2009. Increased transepidermal water loss and decreased ceramide content in lesional and non-lesional skin of dogs with atopic dermatitis. Veterinary Dermatology 20, 541–546.
Sperling, P., Heinz, E., 2003. Plant sphingolipids: Structural diversity, biosynthesis, first genes and functions. Biochimica et Biophysica Acta 1632, 1–15.
Stahl, J., Paps, J., Baümer, W., Olivry, T., 2012. Dermatophagoides farina house dust mite allergen challenges reduce stratum corneum ceramides in an experimental dog model of acute atopic dermatitis. Veterinary Dermatology 6, 497–e97.
Swartzendruber, D.C., Wertz, P.W., Madison, K.C., Downing, D.T., 1987. Evidence that the corneocyte has a chemically bound lipid envelope. Journal of Investigative Dermatology 88, 709–713.
Swartzendruber, D.C., Wertz, P.W., Kitko, D.J., Madison, K.C., Downing, D.T., 1989. Molecular models of the intercellular lipid lamellae in mammalian stratum corneum. Journal of Investigative Dermatology 92, 251–257.
t'Kindt, R., Jorge, L., Dumont, E., Couturon, P., David, F., Sandra, P., Sandra, K., 2012. Profiling and characterizing skin ceramides using reversed-phase liquid chromatography-quadrupole time-of-flight mass spectrometry. Analytical Chemical 84, 403–411.
Tokudome, Y., Uchida, R., Yokote, T., Todo, H., Hada, N., Kon, T., Yasuda, J., Hayashi, H., Hashimoto, F., Sugibayashi, K., 2010. Effect of topically applied sphingomyelin-based liposomes on the ceramide level in a three-dimensional cultured human skin model. Journal of Liposome Research 20, 49–54.
van der Kloet, F.M., Bobeldijk, I., Verheij, E.R., Jellema, R.H., 2009. Analytical error reduction using single point calibration for acute and precise metabolomic phenotyping. Journal of Proteome Research 8, 5132–5141.
van Smeden, J., Hoppel, L., van der Heijden, R., Hankemeier, T., Vreeken, R.J., Bouwstra, J.A., 2011. LC/MS analysis of stratum corneum lipids: Ceramide profiling and discovery. Journal of Lipid Research 52, 1211–1221.
Watson, T.D., 1998. Diet and skin disease in dogs and cats. Journal of Nutrition 12, 2783S–2789S.
Welss, T., Basketter, D.A., Schröder, K.R., 2004. In vitro skin irritation: Facts and future. State of the art review of mechanisms and models. Toxicology In Vitro 18, 231–243.
Yoon, J.S., Nishifuji, K., Sasaki, A., Ide, K., Ishikawa, J., Yoshihara, T., Iwasaki, T., Yoshihara, T., Iwasaki, T., 2011. Alteration of stratum corneum ceramide profiles in spontaneous canine model of atopic dermatitis. Experimental Dermatology 20, 732–736.
Yoon, J.S., Nishifuji, K., Ishioroshi, S., Ide, K., Iwasaki, T., 2013. Skin lipid profiling in normal and seborrhoeic Shih tzu dogs. Veterinary Dermatology 1, 84–89.